Proc. Estonian Acad. Sci. Eng., 2000, **6**, 1, 14–24
https://doi.org/10.3176/eng.2000.1.02

THE INFLUENCE OF TARGET SURFACE ALTERATIONS ON PULSED LASER DEPOSITED $YBa_2Cu_3O_{7-x}$ FILM PROPERTIES

Vitali PODGURSKI

Institute of Materials Technology, Tallinn Technical University, Ehitajate tee 5, 19086 Tallinn, Estonia; povi@edu.ttu.ee

Received 11 September 1998; in revised form 8 April 1999

Abstract. This research focuses on the dependence of laser deposited $YBa_2Cu_3O_{7-x}$ film properties on the depth of ablated target layers. The results demonstrate that the critical temperature T_c, the second phase, and the morphology of the films are sensitive to the conditions of the target. The effect of laser glazing of the target is considered. In the case of thin films, T_c enhancement of the films deposited from the glazed target were observed.

Key words: laser glazing, YBCO, films.

1. INTRODUCTION

The superconductivity of $YBa_2Cu_3O_{7-x}$ (YBCO) thin films is related to the stoichiometry, surface morphology, film thickness as well as to the number, type, and orientation of the defects. On the other hand, laser energy density, laser spot size, substrate–target distance, substrate temperature, oxygen pressure, and target morphology have a significant effect on these film properties [1].

In various applications, smooth YBCO films are required, but defects and inclusions may act as pinning centres raising the critical current density. Therefore, a reasonable compromise between electrical and morphological properties of YBCO films has to be achieved. Recently, different laser deposition arrangements of target versus substrate [2,3], velocity filters, and the use of O_2/Ar atmosphere [4] were proposed in order to obtain droplet- and outgrowth-free surface of thin films.

This work was motivated by the effect of laser-induced chemical and morphological changes on the target surface during laser ablation [5,6].

Alterations in the target surface depend mainly on the influence of the laser, on the number of pulses incident on the target, on the roughness of the "fresh" target, and on the laser spot size. It is well known that changes in the target surface result in various defects in the film. To investigate these influences, a series of films were deposited in succession from the same target.

To modify the target surface, usual sanding was used. As described in [1], laser glazing produces a smoother target surface reducing the collision and hydrodynamic mechanisms of particle formation. Moreover, due to the existence of the surface segregation mechanism [1], the chemical processes on the target surface must be taken into account.

2. EXPERIMENTAL

A KrF excimer laser (Lambda Physics) was employed, with the wavelength of 248 nm, pulse width of 30 ns, and repetition rate of 10 Hz. The laser radiation density on the rotated target surface was 1.2 J/cm^2. The films were deposited on two-side polished (001) oriented $LaAlO_3$ substrates at the on-axis geometry. The substrate–target distance was 60 mm. The substrate was heated up to 780 °C. For all films, during deposition, the partial pressure of oxygen was 0.6 mbar and during cooling, 9×10^2 mbar. The cooling rate was 60 K/min.

The first five films were deposited from a single laser polished target. The target was sanded and irradiated at about 0.04 J/cm^2 during 2 min at 1 Hz. During this process the whole target surface was under radiation. First, film N1, then without any polishing of the target, film N2, up to the N5 were deposited. Films N6 and N7 were prepared in the same way, with the exception that the target was only sanded before the deposition process. In the case of films N1 to N7, the target was exposed to 1800 pulses for each film. Film N8 was deposited during 9000 pulses from a single target without previous glazing. For film N9, 9000 pulses were produced from five different targets, each one glazed as described above.

X-ray diffraction (XRD) measurements were carried out on the Philips and Siemens D-5000 diffractometers. Droplets and surface morphology were examined, using the scanning electron microscopy (SEM). The chemical composition of films N8 and N9 was determined by the Secondary Ion Mass Spectroscopy (SIMS).

3. RESULTS AND DISCUSSION

Figure 1 indicates that the film N1 has higher T_c than the film N6, produced from the sanded target. The resistivity curve of transition shows that two superconductive phases are present for film N1 (Figs. 2 and 3), but only one

exists for the film N6. This clearly indicates the presence of the glazing effect. However, this effect disappears for the film N9. The T_c of the films N8 and N9 was 89 K and the transition width was 0.2 K.

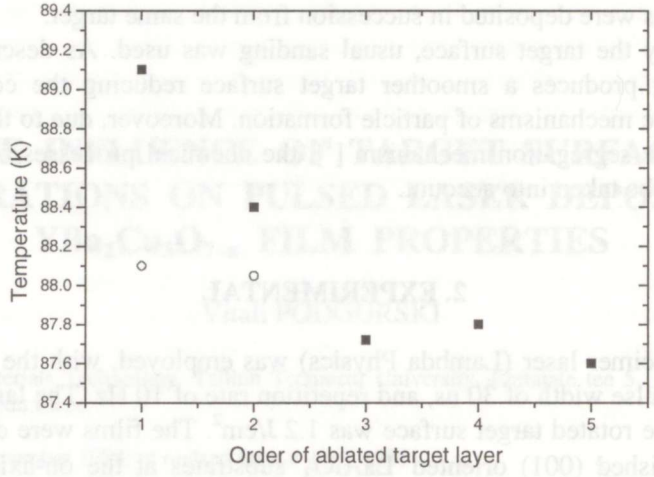

Fig. 1. Temperature of phase transitions vs order of ablated target layer: ■ – films N1–N5; ○ – films N6 and N7.

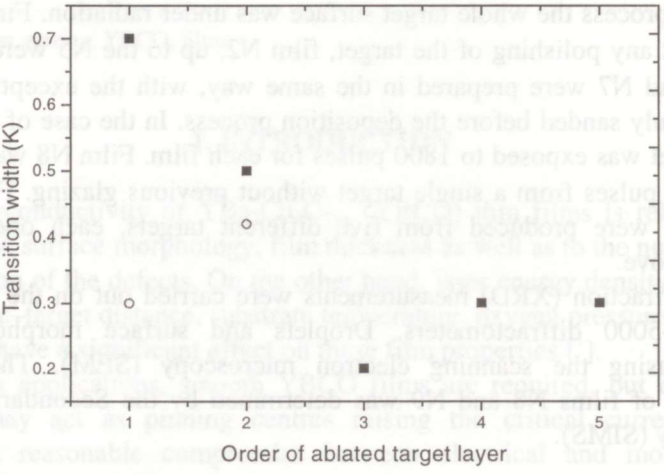

Fig. 2. Transition width vs order of ablated target layer: ■ – films N1–N5; ○ – films N6 and N7.

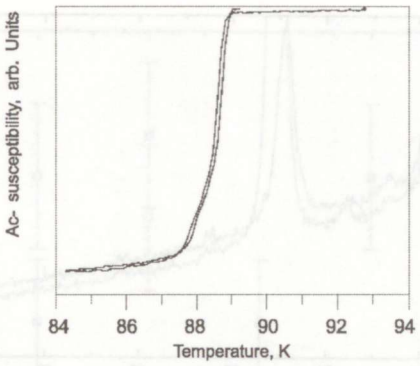

Fig. 3. Ac-susceptibility transitions vs temperature for the film N1.

Besides strong c-axis texturing, as measured by XRD, additional second phase peaks were observed. The most prominent peaks were the following (Figs. 4 and 5): two Cu_2O peaks at $2\theta = 61.38°$, (220) reflection, and at $2\theta = 29.59°$, (110) reflection; the peak of Y_2O_3 at $2\theta = 33.7°$, (004) reflection [7], and probably the peak of $Y_2Cu_2O_5$ at $2\theta = 51.85°$, (414) reflection. The Cu_2O had cubic Pn3m symmetry and the ratio of I_{110}/I_{220} was between 1 and 1.5; according to the XRD file JCPDS-ICDD N5-667, this ratio is 3. In addition, two weak CuO peaks are present at $2\theta = 83.1°$, (222) reflection, and probably at $2\theta = 58.2°$, (101) reflection [8]. These data indicate that at least two reactions are possible. First, Cu_2O and O_2 react to form CuO. This reaction can be present during the film cooling and oxidation [8]. Second, the reaction

$$Y_2O_3 + Cu_2O + 1/2O_2 \rightarrow Y_2Cu_2O_5$$

can occur under oxidizing conditions only [9].

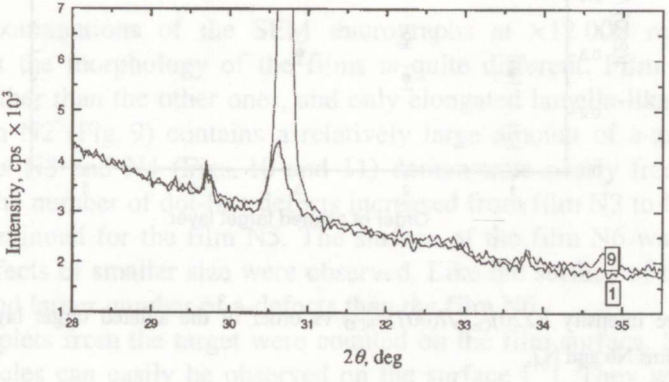

Fig. 4. XRD data for films N1 and N9 recorded with 0.1° offset.

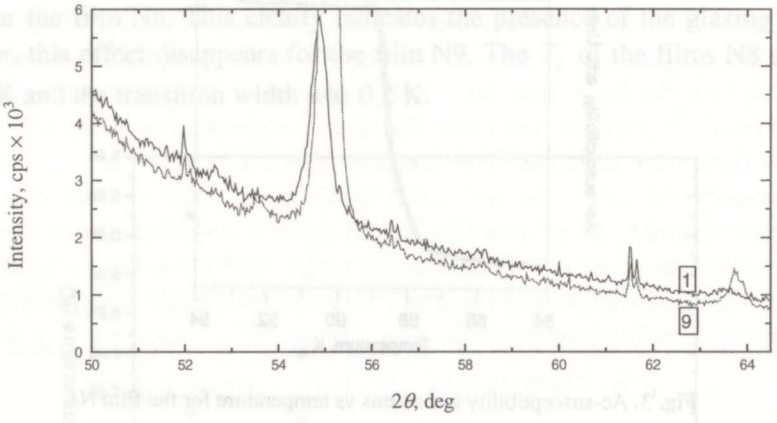

Fig. 5. XRD data for films N1 and N9 recorded with 0.1° offset.

The relative volume ω_1 of Cu_2O in YBCO films (Fig. 6) was estimated by comparing the intensities of Cu_2O, (220) reflection and (007) reflection of YBCO, and ω_2 (Fig. 7) of CuO, (222) reflection, and (00.10) reflection of YBCO; $\omega = I_{SP}/I_{YBCO}$ where I_{SP} is the intensity of the second phase peak and I_{YBCO} is the intensity of the seventh or tenth peak of YBCO.

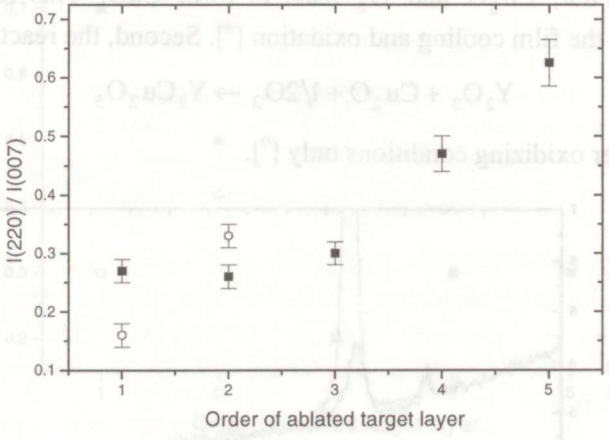

Fig. 6. Relative intensity $I(220)_{Cu_2O}/I(007)_{YBCO}$ vs order of the ablated target layer: ■ – films N1–N5; ○ – films N6 and N7.

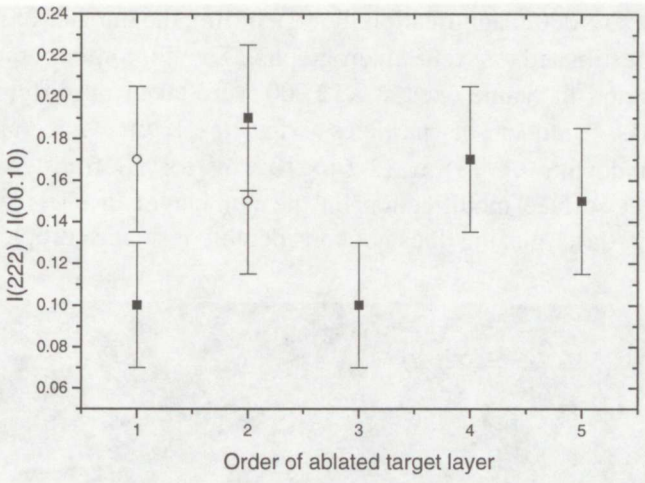

Fig. 7. Relative intensity $I(222)_{CuO}/I(00.10)_{YBCO}$ vs order of the ablated target layer: ■ – films N1–N5; ○ – films N6 and N7.

The size of the error bars was determined according to

$$\Delta\omega = \sqrt{\frac{I_{SP}}{I_{YBCO}^2} + \frac{I_{SP}^2}{I_{YBCO}^3}}.$$

For the films N8 and N9, $\omega_1 = 0.05$ and $\omega_2 = 0.01$. Relatively higher ratios of ω_1 of the samples N4 and N5 in comparison with those of N1, N2, and N3 indicate the increasing amount of Cu_2O at the increasing depth of the ablated target layer. However, in the case of ω_2, such behaviour does not occur any longer.

Planar examinations of the SEM micrographs at ×12 000 magnification indicate that the morphology of the films is quite different. Film N1 (Fig. 8) seems smoother than the other ones, and only elongated lamella-like defects are visible. Film N2 (Fig. 9) contains a relatively large amount of a-axis oriented grains. Films N3 and N4 (Figs. 10 and 11) demonstrate nearly free a-oriented grains, but the number of dot-like defects increased from film N3 to N4, and this tendency continued for the film N5. The surface of the film N6 was similar to N1, only defects of smaller size were observed. Like the surface of the film N2, that of N7 had larger number of a-defects than the film N6.

Only droplets from the target were counted on the film surface. Spherically-shaped particles can easily be observed on the surface [10]. They were divided into two categories: droplets $d > 1$ μm, which can be identified on the SEM micrographs at ×700 magnification and droplets $d < 1$ μm, which are

identifiable at ×12 000 magnification. For each film, the number of both kinds of droplets was estimated on four micrographs. The four micrographs at ×700 magnification and the same ones at ×12 000 were taken on different places of the films. The number of particles with $d < 1$ μm were approximately $5 \times 10^5/\text{cm}^2$ and with $d > 1$ μm, $(2–6) \times 10^4/\text{cm}^2$ for all films. No noticeable effect of target surface modification on the number of droplets was observed and, apparently, laser glazing does not considerably influence droplet formation.

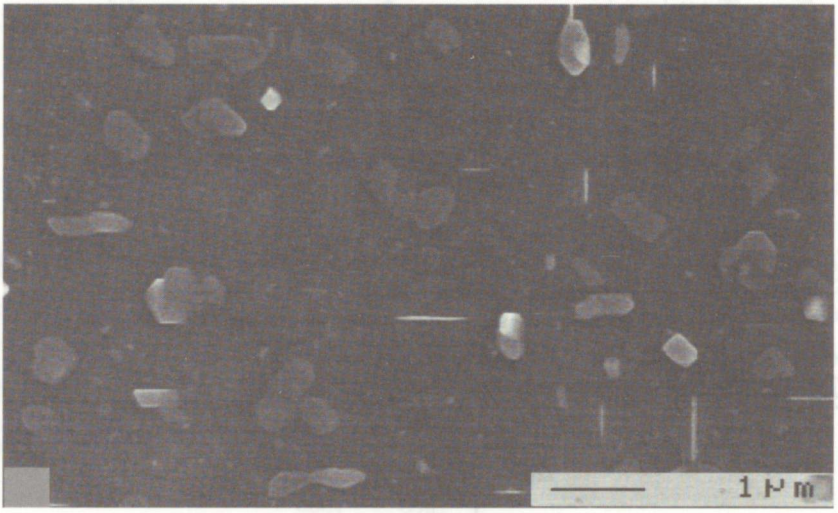

Fig. 8. SEM micrograph of the film N1.

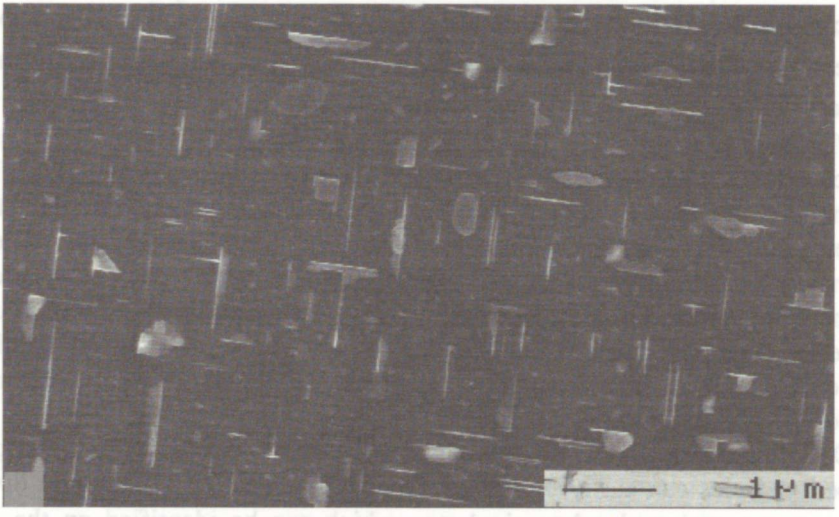

Fig. 9. SEM micrograph of the film N2.

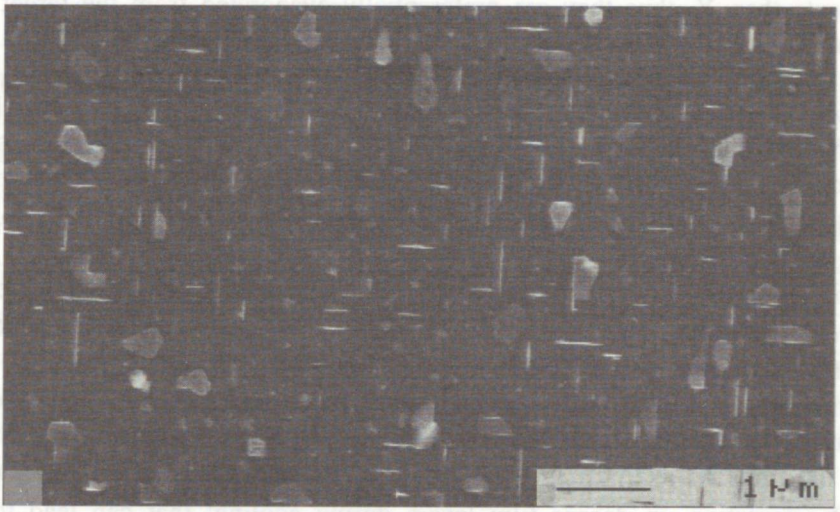

Fig. 10. SEM micrograph of the film N3.

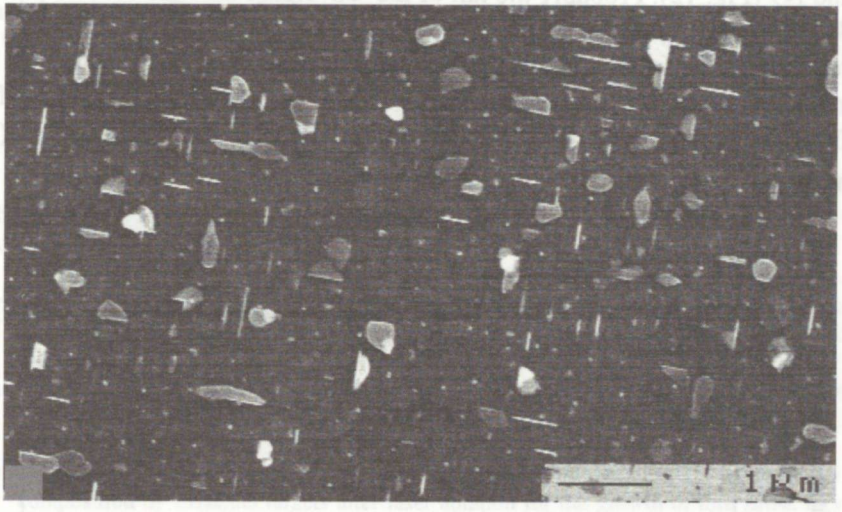

Fig. 11. SEM micrograph of the film N4.

It is worth to emphasize some issues related to the common mechanisms of film growth and to the formation of the second phases. First, the amount of each element can be regarded as composed of three parts: (1) the part re-evaporated from the film, (2) that forming the YBCO phase, and (3) that contained in the second phases formed either in reactions between simpler compounds or by the decomposition of complex compounds. Second, Ba and Cu are more volatile

elements than Y, thus they are preferentially evaporated from the target and probably from the film surface due to high substrate temperature. Third, the target surface composition changes from 1-2-3 to Y-rich [6]. Fourth, long distance from the target to the substrate causes deficient Ba and Y, and rich Cu [10]. Since Cu has the highest velocity and smallest size, it can reach the substrate without scattering at high pressure O_2. Based on the considerations above and on the conditions of the experiment, it is very likely that all films are Ba-deficient and Cu-rich.

In the case of Cu, CuO is affected by cooling and oxidation and, apparently, it grows prevalently on the surface; inside the film, the growth of CuO is diminished. The amount of CuO (111) in thick films N8 and N9 is smaller than in thin films, at least for one order. It should be noticed that the time and the cooling conditions were identical for all films. As films N8 and N9 are thicker than the films N1–N7, Cu_2O cannot be easily transformed to CuO, at least of (111) orientation, in deeper film layers during cooling; that can lead to the decreasing ratio of I_{CuO}/I_{YBCO}. The nearly invariable ω within the error bars for thin films N1–N7 supports it. Indirect evidence of preferential formation of Cu-rich defects in the upper film layers is shown by the SIMS profiles of the films N8 and N9 (Fig. 12). Probably the tail of the Cu signal near the surface is due to CuO and Cu-rich defects.

In [8] the influence of different substrates on the orientation of CuO has been described. It has been found that strongly (111) oriented CuO is very specific to MgO (001) substrates, while the film on $LaAlO_3$ has weak peak (101) orientation. The results of the present work are in agreement with the latter.

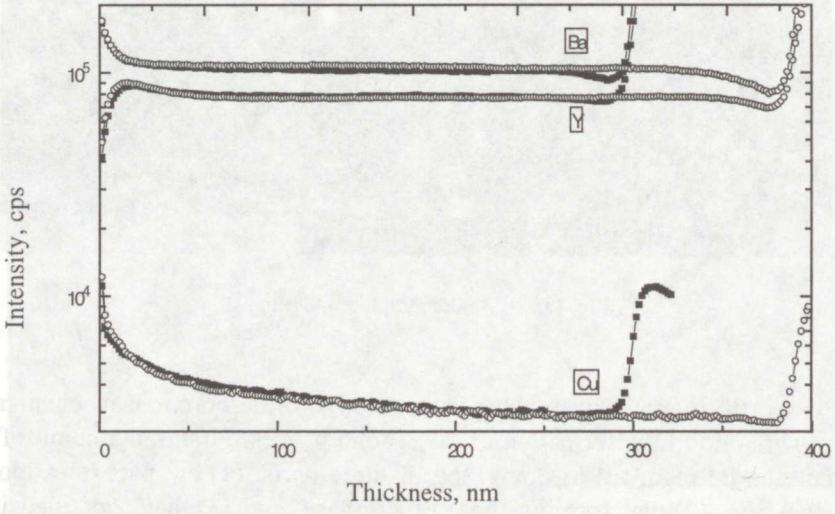

Fig. 12. SIMS spectrum (in-depth profile): ■ – film N8; ○ – film N9.

4. CONCLUSIONS

This study describes the influence of the compositional and morphological variations of the laser-induced target on film properties. It has been found that T_c and the morphology of the films are sensitive to the depth of the irradiated target layer. The effect of target glazing has been considered. During the first 5400 pulses, T_c of the films made in succession from the glazed target showed a rapid decrease and a subsequent stabilization. In the case of Cu_2O, XRD measurements demonstrated an increase in the aspect ratio of I_{Cu_2O}/I_{YBCO} for thin films deposited from deeper target layers. Based on the XRD and SIMS measurements, we can conclude that CuO, at least of (111) orientation, prevalently forms close to the film surface.

ACKNOWLEDGEMENTS

The author is grateful to T. Claeson for offering an opportunity to conduct this research, and to the Swedish Institute and the Johnson Foundation for their financial support. The author also wishes to thank Z. Ivanov, L. Vratislav, and P. B. Mozhaev for fruitful discussions and M. Friesel for the SIMS observation.

REFERENCES

1. Chrisey, D. and Hubbler, G. *Pulsed Laser Deposition of Thin Films*. J. Wiley, New York, 1994.
2. Holzapfel, B., Roas, B., Schultz, L., Bauer, P., and Saemann-Ischenko, G. Off-axis laser deposition of $YBa_2Cu_3O_{7-\delta}$ thin films. *Appl. Phys. Lett.*, 1992, **61**, 26, 3178–3182.
3. Trajanovic, Z., Senapati, L., Sharma, R., and Venkatesan, T. Stoichiometry and thickness variation of $YBa_2Cu_3O_{7-x}$ in off-axis pulsed laser deposition. *Appl. Phys. Lett.*, 1995, **66**, 18, 2418–2424.
4. Kuhle, A., Skov, J., Hjorth, S., Rasmussen, I., Bindslev, T., and Hansen, J. Smooth $YBa_2Cu_3O_{7-x}$ thin films prepared by pulsed laser deposition in O_2/Ar atmosphere. *Appl. Phys. Lett.*, 1994, **64**, 23, 3178–3182.
5. Andreouli, C., Christoulakis, S., Tsetsekou, A., and Efthmiopoulos, T. Morphology and composition of YBaCuO targets after laser ablation for the growth of thin films. *Key Eng. Mater.*, 1997, **132–136**, 2, 1281–1284.
6. Young, K. H. Morphology and composition of YBaCuO targets after long period laser ablation. *Physica C*, 1993, **211**, 1, 1–12.
7. Selinder, T., Helmersson, U., Han, Z., and Wallenberg, L. Structural characterisation of yttria (Y_2O_3) inclusions in $YBa_2Cu_3O_{7-x}$ films: Growth model and effect on critical current density. *Thin Solid Films*, 1993, **229**, 2, 237–247.
8. Watson, I., Atwood, M., and Gumberbatch, J. Triaxially oriented growth of CuO on MgO (001): X-ray diffraction studies of pure CuO films and inclusions in superconducting Y–Ba–Cu–O films prepared by MOCVD. *Thin Solid Films*, 1994, **251**, 1, 51–62.
9. Eibl, O. and Roas, B. Microstructure of $YBa_2Cu_3O_{7-x}$ thin films deposited by laser evaporation. *J. Mater. Res.*, 1990, **5**, 3, 2620–2632.

10. Proyer, S., Stangl, E., Borz, M., Hellebrand, B., and Bauerle, D. Particulates on pulsed-laser deposited Y–Ba–Cu–O films. *Physica C*, 1996, **257**, 1/2, 1–15.

MÄRKLAUA KOOSTISE MÕJU IMPULSSLASERIGA SADESTATUD $YBa_2Cu_3O_{7-x}$ KILEDE OMADUSTELE

Vitali PODGURSKI

On käsitletud märklaua koostise ja morfoloogia mõju kilede omadustele laserpindamisel. Kile morfoloogia ja kriitiline temperatuur T_c sõltuvad märklaua aurustatava materjali kiiritatava kihi sügavusest. Juhul kui kiled sadestatakse märklauast, mis on eelnevalt poleeritud laserkiirgusega, langeb T_c kiiresti esimese 5400 impulsi järel ning stabiliseerub siis. Uuringud röntgendifraktsiooni meetodil näitasid, et suhe I_{Cu_2O}/I_{YBCO} kasvab kiledel, mis on sadestatud märklaua sügavamatest kihtidest. On selgitatud, et CuO kristallograafiline tasand (111) formeerub peamiselt kile pinna lähedal.